Utilizing Furfural-based Bifuran Diester as Monomer and Comonomer for High-Performance Bioplastics: Properties of Poly(butylene furanoate), Poly(butylene bifuranoate), and their Copolyesters

Utilizing Furfural-based Bifuran Diester as Monomer and Comonomer for High-Performance Bioplastics: Properties of Poly(butylene furanoate), Poly(butylene bifuranoate), and their Copolyesters

Tuomo P. Kainulainen,[a] *Terttu I. Hukka,*[b] *Hüsamettin D. Özeren,*[c] *Juho A. Sirviö,*[d] *Mikael S. Hedenqvist,*[c] *Juha P. Heiskanen*,*[a]

[a]Research Unit of Sustainable Chemistry, University of Oulu, P.O. Box 4300, FI-90014 Oulu, Finland

[b]Laboratory of Chemistry and Bioengineering, Tampere University of Technology, P.O. Box 541, FI-33101 Tampere, Finland

[c]Department of Fibre and Polymer Technology, School of Engineering Sciences in Chemistry, Biotechnology and Health, KTH Royal Institute of Technology, SE-100 44, Stockholm, Sweden

[d]Fibre and Particle Engineering Research Unit, University of Oulu, P.O. Box 4300, FI-90014 Oulu, Finland

Abstract

Two homopolyesters and a series of novel random copolyesters were synthesized from two bio-based diacid esters, dimethyl 2,5-furandicarboxylate, a well-known renewable monomer, and dimethyl 2,2'-bifuran-5,5'-dicarboxylate, a more uncommon diacid based on biochemical furfural. Compared to homopolyesters poly(butylene furanoate) (PBF) and poly(butylene bifuranoate) (PBBf), their random copolyesters differed dramatically in that their melting temperatures were either lowered significantly or they showed no crystallinity at all. However, the thermal stabilities of the homopolyesters and the copolyesters were comparable. Based on tensile tests from amorphous film specimens, it was

concluded that the elastic moduli, tensile strengths, and elongation at break values for all copolyesters were similar as well, irrespective of the furan:bifuran molar ratio. Tensile moduli of approximately 2 GPa and tensile strengths up to 66 MPa were observed for amorphous film specimens prepared from the copolyesters. However, copolymerizing bifuran units into PBF allowed the glass transition temperature to be increased by increasing the amount of bifuran units. Besides enhancing the glass transition temperatures, the bifuran units also conferred the copolyesters with significant UV absorbance. This combined with the highly amorphous nature of the copolyesters allowed them to be melt-pressed into highly transparent films with very low ultraviolet light transmission. It was also found that furan-bifuran copolyesters could be as effective, or better, oxygen barrier materials as neat PBF or PBBf, which themselves were found superior to common barrier polyesters such as PET.

Keywords: Barrier, Copolyester, Furan, Renewable

Introduction

Scheme 1. Furan-based polyesters as potential alternatives for current commodity polyesters

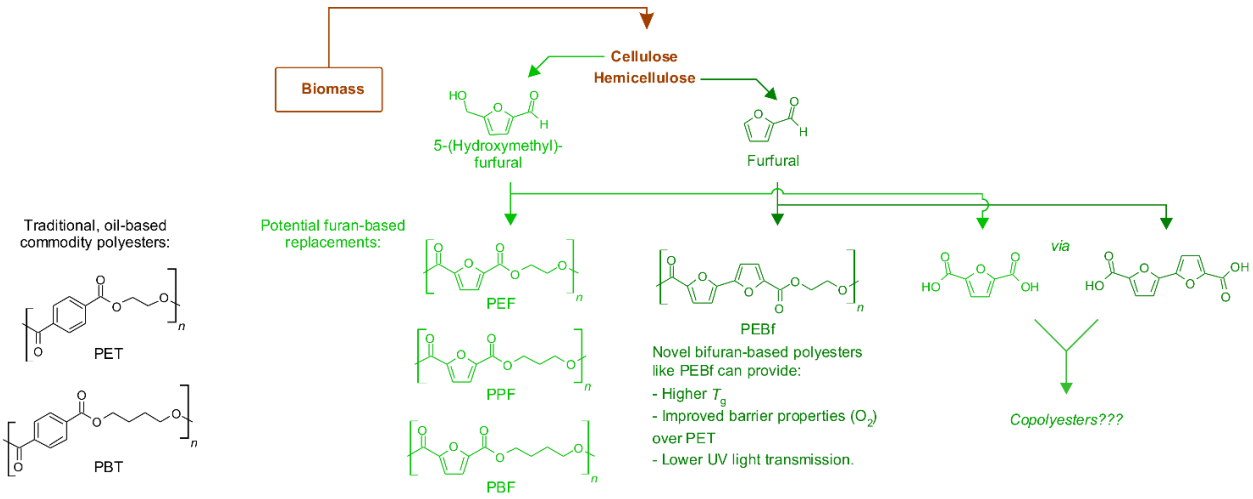

Use of biomasses as alternative feedstocks for chemicals is one of the most important aspects of reducing dependence on fossil-based resources.[1] Furans are key bio-based platform-chemicals, as they are readily prepared from monosaccharides, which plant-based biomasses contain in large quantities as two important polymerized forms, i.e. cellulose and hemicellulose.[2] Moreover, many

industrial and agricultural processes result in by-products, e.g. sugar-cane bagasse or corncobs that are rich in cellulose and hemicellulose. After depolymerization, their C5 and C6 sugars can be readily dehydrated into two important furans, furfural and 5-(hydroxymethyl)furfural (HMF), respectively (Scheme 1).[3,4] Furfural is especially notable, as its commonly derived from the inedible, C5 sugar containing hemicellulose byproducts of various crops; the industrial production of furfural has been ongoing since the 1920s.[5] The first processes used leftover oat hulls as the feedstock and provided a way to valorize a "waste" biomass into furfural, which is a highly useful chemical intermediate.

Lately, the focus has been on HMF, as it is one of the chief precursors to 2,5-furandicarboxylic acid (FDCA).[6] Notably, HMF can be directly oxidized into FDCA, whereas additional steps are necessary to convert furfural into FDCA.[7,8] FDCA continues to attract considerable interest due to its similarity with terephthalic acid (PTA), which in turn is the precursor to the commodity polyester poly(ethylene terephthalate) (PET).[9,10] Excellent properties of PET have made it especially prevalent in packaging, and replacing polyesters like PET with furan-based alternatives could help reduce the environmental impact of non-renewable packaging plastics, which are under high demand.[11] Another important commodity polyester based on PTA is poly(butylene terephthalate) (PBT). It is more commonly used in manufacture of molded articles where the rapid crystallization of PBT melts is a benefit.[12] The faster crystallization is made possible by the replacement of the stiffer ethylene chain in PET with a more flexible butylene chain in PBT. However, well-known, widely used technical plastics such as PET and PBT are not easily displaced by new biomass-based alternatives. For this reason, methods for producing terephthalic acid from biomass-based routes, including conversion of furfural[13], have been studied and reviewed.[14] It has been estimated that some bio-based routes to terephthalic acid might become feasible soon, and that they could reduce the environmental impact when compared to the use of non-renewable sources.[15]

Still, the straightforward nature of simple furans makes them interesting as bio-based aromatic polymer precursors. Moreover, FDCA-based polyesters possess value beyond simply their biomass

origin. In a relatively short time, the potential of furan compounds as precursors for new high-performance yet renewable materials has become evident: Poly(ethylene furanoate) (PEF)[16,17,18], poly(propylene furanoate) (PPF)[19], and poly(butylene furanoate) (PBF)[20] have been shown to far exceed the performance of PET in terms of gas permeability. For example, PEF has been reported to provide 11x and 19x reductions in oxygen and carbon dioxide permeabilities, respectively, when compared to PET, potentially enabling furan-based packaging materials with performance improvements. Reduced permeability can increase the shelf life of foods and beverages, for instance, and enable the use of thinner and lighter packaging. Thus, the potential of furan compounds as precursors for new high-performance yet renewable materials has become evident.

Recently, the use of 2,2'-bifuran-5,5'-dicarboxylic acid (BFDCA) as a precursor for novel bio-based polyesters has been described.[21,22] In addition to this, it has only been demonstrated as a precursor for novel polyamides.[23] BFDCA can be regarded as a furfural-derived C10 monomer with planar biheteroaryl core, which sets it apart from not only FDCA and PTA but also many other bio-based bicyclic monomers as well. Polyesters incorporating bio-based bicyclic structures with aliphatic structures[24,25,26,27], especially from isosorbide, are relatively well-known whereas bicyclic aromatic examples are scarcer and more singular, e.g. indole-based polyesters[28]. The use of bicyclic monomers is in large part motivated by their inherent rigidity compared to e.g. linear acyclic monomers, thus usually leading to polymers with enhanced T_g. Our preliminary investigation showed that BFDCA-based polyester poly(ethylene bifuranoate) (PEBf) has higher glass-transition temperature than PET and PEF, meaning BFDCA-based polyesters should maintain higher rigidity at elevated temperatures. In addition, the highly conjugated molecular structure of BFDCA also inherently provides polyesters with stronger UV light absorption, again setting it apart from more common bio-based monomers.[22] Limited data is available on the barrier properties of bio-derived polyesters containing other rigid bicyclic structures such as isosorbide, with one such study concerning copolyesters based on poly(butylene succinate) (PBS) that incorporated isosorbide units.[29] The results suggested that the

effect of the isosorbide units can depend on the unit content: The stiffness of isosorbide moieties at low content (11 mol%) resulted in reduced oxygen permeability, while higher contents reduced crystallinity to the point that an increase in oxygen permeability occurred with respect to PBS. In our investigation, PEBf possessed lower O_2 and water vapor permeability than a comparable PET sample, hinting that bifuran units could be helpful in reducing gas permeability. Due to the initial promise shown by BFDCA as a new bio-based monomer, it could offer a novel way of utilizing furfural as a feedstock for high-performance bioplastics.

In this paper, the synthesis of new random copolyesters of poly(butylene furanoate) (PBF) and poly(butylene bifuranoate) (PBBf), derived from FDCA and BFDCA, respectively, are presented. Thermal and mechanical properties of the copolyesters are then compared to the pure homopolyesters derived from FDCA and BFDCA. Specifically, it is shown that having either FDCA or BFDCA as the minor comonomer can significantly influence the crystallinity of the resulting copolyester. However, it is also shown that potentially beneficial UV filtering property can be realized in FDCA-based polyesters incorporating some BFDCA as the minor component. This allows for crystallizability from PBF to be retained to some extent. Additionally, the copolyesters are shown to have promise as excellent barrier against oxygen, much like PBF and PBBf, despite their more amorphous nature.

Experimental

1,4-Butanediol was distilled under reduced pressure onto 3Å molecular sieves prior to use. Otherwise, commercially available solvents were used as received. ^{1}H NMR chemical shifts are referenced to residual solvent peaks in TFA-*d* and $CDCl_3$ at 11.50 and 7.27 ppm, respectively. ^{13}C NMR shifts were referenced to the trifluoromethyl carbon (116.60 ppm, $F_3\underline{C}COOD$) in TFA-*d*. All NMR measurements were carried out at room temperature.

Dimethyl 2,5-furandicarboxylate (**1**): 2,5-Furandicarboxylic acid (4.00 g, purity 98%) was refluxed in large excess of dry methanol (120 mL) overnight with concentrated sulfuric acid (2 equiv) under

argon. The cooled mixture was then partially evaporated to about 1/3–1/2 volume and diluted with cold deionized water to precipitate the product. After filtration and drying in air, the raw product was dissolved in ethyl acetate and passed through a layer of silica gel. After evaporation of the solvent, dimethyl 2,5-furandicarboxylate (4.25 g, 93%) was collected as a white powder. ^{1}H NMR (400 MHz, $CDCl_3$, ppm): δ 7.23 (s, 2H), 3.94 (s, 6H).

Dimethyl 2,2'-bifuran-5,5'-dicarboxylate (**2**): The synthesis method we reported previously was followed to afford dimethyl 2,2'-bifuran-5,5'-dicarboxylate (4.53 g, 91%) as small white needles.[22] ^{1}H NMR (400 MHz, $CDCl_3$, ppm): δ 7.26 (d, 2H, J = 3.7 Hz), 6.90 (d, 2H, J = 3.7 Hz), 3.93 (s, 6H).

Polyester synthesis: The polyesters were synthesized by weighing the appropriate amount of diester(s) (8 mmol total) into a 50 mL round-bottom flask equipped with a magnetic stirring bar. 1,4-Butanediol (3 equiv) was added, together with tetrabutyl titanate (0.1 mol% relative to the total diester amount) dissolved in small amount of dry toluene (0.03 M). The flask was connected to a short-path type distillation bridge and the reaction system was evacuated and filled with argon gas. After five evacuation and filling cycles, the flask was heated to 180 °C using an aluminium heating block. After 3 h, the pressure was gradually lowered to 2 mbar over 1 h. Then, the temperature of the system was increased to 250 °C to initiate the polycondensation and distill off 1,4-butanediol from the flask. After 1 h, the polycondensation was stopped, and the cooled polyester was allowed to dissolve in a mixture of trifluoroacetic acid (TFA) and chloroform (1:5 v/v). The polyester solution (approx. 0.1 g/mL) was then slowly mixed into 10-fold excess of methanol to yield white-to-off white fibrous solid. After filtration onto paper, the fibrous solid was rinsed with methanol, and gently pressed dry. Final drying was accomplished under vacuum at 60 °C to a constant weight. For ^{1}H and ^{13}C NMR, 5–10 mg of polyester was dissolved in ca. 0.4 mL of deuterated trifluoroacetic acid or $CDCl_3$-TFA mixture (approx. 3:1 v/v). For proton decoupled ^{13}C NMR measurements, 1000–5000 scans were collect with acquisition time of 1.4 s.

Dilute solution viscometry: Intrinsic viscosities were determined from flow times of pure TFA (t_0) and filtered polyester solutions (0.5 g/dL) in TFA (t) in a micro-Ubbelohde viscometer submerged in 30.0 °C water bath. The average of ten flow times were used to calculate t_0 and t.

ATR-FTIR: The vibrational properties of the polymer samples were analyzed using Perkin Elmer Spectrum One FT-IR Spectrometer with the attenuated total reflection (ATR) technique in the wavelength region of 650–4000 cm^{-1}, resolution of 2 cm^{-1}, accumulation of eight scans, in transmission mode.

Differential scanning calorimetry (DSC): Differential scanning calorimeter (Mettler Toledo DSC 821e and DSC1) was used to investigate the phase transition temperatures at the range of 25–300 °C with heating and cooling rates of 10 °C/min under nitrogen (N_2) gas flow (60 cm^3/min). The polymer samples (ca. 5 mg), were placed into 40 μL Al crucibles sealed with pierced lids. Thermal history was deleted by the first heating.

Thermogravimetric analysis (TGA): Decomposition properties and thermal stability of the polymer samples (ca. 10 mg) were studied with a thermogravimetric analyzer (Mettler-Toledo TGA851e). Samples were placed into a 70 μL Al_2O_3 crucible, which was covered with a pierced lid and heated from 30 to 700 °C under nitrogen flow (95 cm^3/min) using a heating rate of 10 °C/min.

Melt hot pressing: Dried polymer samples were melt-pressed into films suitable for characterization of mechanical performance and barrier properties. Two aluminium plates coated with thin polyimide film were used for the pressing, with the appropriate amount of polyester added between the pre-heated plates. The thickness was controlled using layers of glass fiber mat placed around the sample. The polyesters were first allowed to melt inside the press at temperatures 20–30 °C above their expected melting temperatures (listed in Table 1, e.g. 160 °C for $PBF_{50}Bf_{50}$) for 5 minutes. 20 kN pressing force was then applied for 1 minute. The samples were cooled inside the press with an integrated water-cooling circuit (cooling rate approx. 30–40 °C/min) to provide low-crystallinity

films. The plates were then carefully separated, and the films were peeled off to yield flexible, transparent films. ^{1}H NMR samples were also prepared from pressed films to observe possible chemical changes.

Tensile testing: Tensile test specimens were rectangle-shaped, with 5 mm width and thicknesses between 100–200 μm. The specimens were stored at room temperature for 1–2 weeks prior to the uniaxial tensile tests and a further 48 h under stable conditions (23 °C, 10% RH) before the tensile tests. The tensile tests were conducted under the same conditions. Tensile modulus, tensile strength and elongation at break were measured (Instron 5544, USA) using a gage length of 30 mm and crosshead speed of 5 mm/min.

Dynamic mechanical analysis: The dynamic mechanical properties were obtained in tensile mode using a DMA Q800 (TA Instruments, USA). Samples with a size of 20×5 mm^2 were used. All runs were performed in a "multi-frequency, strain" mode at 1 Hz, 0.08% strain, from −50 to 120 °C at a heating rate of 3 °C/min with a 15 mm gauge length.

Gas permeability analysis: The oxygen transmission rate (OTR) of the melt-pressed films was measured using a MOCON OxTran 2/20 at 23 °C and 50% RH (relative humidity) with a specimen exposure area of 5 cm^2. Oxygen was then introduced to one surface of the sample at atmospheric pressure. Permeated oxygen was carried away from the downstream surface of the film sample by the carrier gas (N_2). Oxygen permeability (OP) was calculated by multiplying OTR by the thickness of the film and dividing it by the difference in the partial pressure of the oxygen gas between the two sides of the film.

XRD: X-ray diffraction was used to probe crystallinity from the melt-pressed films. Measurements were taken on a PANalytical X'Pert MPD Pro using copper radiation ($K_{\alpha 1}$ = 1.5405980 Å), equipped with an X'Celerator-detector.

UV-vis: Shimadzu UV-1800 spectrophotometer was used to acquire absorption and transmission spectra from melt-pressed films and solutions of monomers **1** and **2**. For both monomers, a 0.01 mg/mL chloroform solution was used to acquire the UV-vis absorption spectra (Figure S15).

Results and Discussion

To prepare the polyesters, dimethyl esters of FDCA (**1**) and BFDCA (**2**) were reacted with 1,4-butanediol in a two-step procedure (reaction scheme in Table 1). The feed ratio of diesters **1** and **2** was adjusted to provide polyesters with the desired molar ratio of furan and bifuran units. Titanium(IV)butoxide (TBT) was added as a catalyst for the reaction, as titanium alkoxides are highly active in both transesterification and polycondensation steps, enabling rapid reactions.[30] Due to the relatively small scale of the reactions (1–2 g) and the low catalyst loading (0.1 mol%), TBT was added as a solution in dry toluene, enabling more accurate metering of the catalyst.

Table 1. Synthesis results for copolyesters

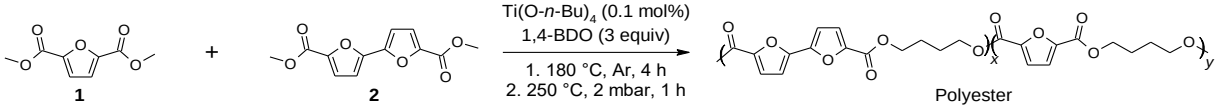

Polyester	Unit ratio, **1**:**2** (mol%)		Yield	IV[b]	Number-average sequence lengths[c]		R_i[c]
	Feed	Product[a]	(%)	(dL/g)	L_{FF}	L_{BB}	
PBF	100:0	100:0	93	0.77	-	0	0
$PBF_{90}Bf_{10}$	90:10	90:10	93	0.95	8.84	1.16	0.98
$PBF_{75}Bf_{25}$	75:25	76:24	95	0.90	3.65	1.38	1.00
$PBF_{50}Bf_{50}$	50:50	51:49	98	0.87	2.08	1.89	1.01
$PBF_{25}Bf_{75}$	25:75	26:74	90	0.67	1.27	4.13	1.03
$PBF_{10}Bf_{90}$	10:90	10:90	91	0.70	1.12	6.94	1.04
PBBf	0:100	0:100	97	0.72	0	-	0

[a]As determined from ^{1}H NMR integrals (TFA-*d*). [b]Intrinsic viscosity evaluated using the Billmeyer relation[31], flow times determined in TFA (30 °C) at a concentration of 0.5 g/dL. [c]Determined by ^{13}C NMR using Equations 1 and 2, randomness index R_i calculated from Equation 3.

In all polycondensation reactions with bifuran **2** present, the melts gradually developed light yellow color during the polycondensation step. After dissolution and precipitation, melt-pressing was used to obtain films with similar light-yellow appearance (Figure 1). In contrast, the PBF melt had practically colorless appearance at the end of the polycondensation, and even the melt-pressed films retained an almost colorless appearance. It seems logical that the increased conjugation and higher

molar extinction coefficient of **2**, when compared to **1**, can result in more intensely colored side-products at elevated temperatures. TBT and similar titanium catalysts are also known to have a tendency to impart color.[30] However, the purity of all synthesized polyesters was comparable based on ^{1}H NMR analysis (Figure 2). Most importantly, the diester feed ratio was accurately reproduced in the final polyesters (Table 1). Thus, both diesters must have similar reactivity and stability under the employed reaction conditions.

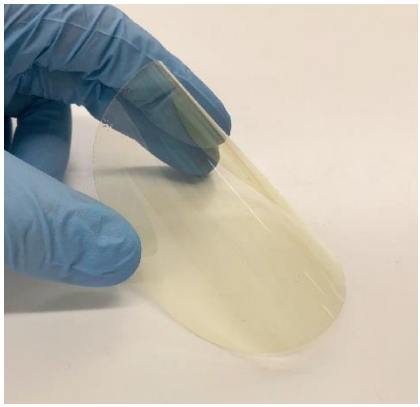

Figure 1. Digital image of a melt-pressed copolyester ($PBF_{90}Bf_{10}$) film.

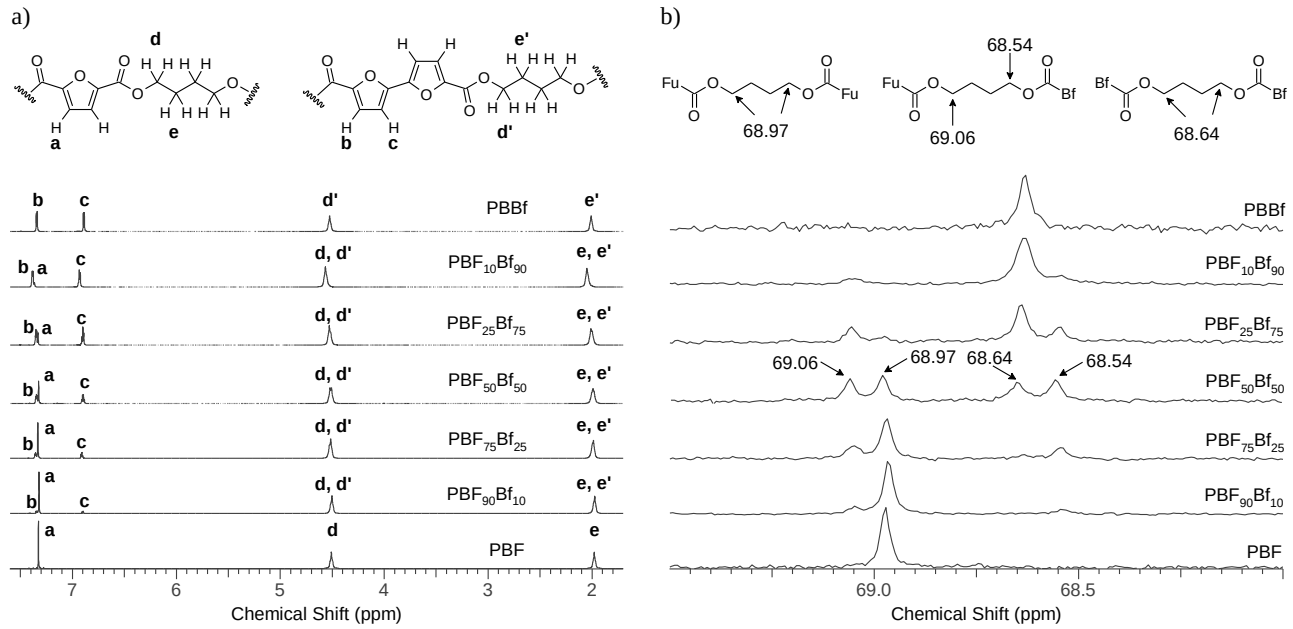

Figure 2. a) ^{1}H NMR signal assignments of the polyesters in TFA-*d*. b) ^{13}C NMR assignment of the sequence sensitive butylene group carbon in TFA-*d* (Fu=furan, Bf=bifuran).

A closer look at the ^{1}H NMR spectra (Figures S3–9 in Supporting Info) reveals convolution by the expected random distribution of furan and bifuran units along the polymer chains. The ^{1}H NMR

spectrum of $PBF_{50}Bf_{50}$, for example, clearly shows that the hydrogen atoms on the furan and bifuran moieties are sensitive to neighboring groups, resulting in overlapping signals and peak broadening (Figure S6). Utilizing ^{13}C NMR, which allows a more detailed analysis due to the broader chemical shift range, a reasonable assignment of the chain structure was obtained (Figure 2b, Table 1). Using areas under the corresponding peaks (A_{FF}, A_{BB}, A_{FB}, and A_{BF}), the number-average sequence lengths of furan (L_{FF}) and bifuran (L_{BB}) segments were estimated (Equations 1 and 2).[32] Previously, such evaluation of sequence distribution was approximated to result in error of ±10%.[32] For the calculations, the four different butylene carbons indicated in Figure 2b were assumed to always provide the same peak areas relative to their abundance. This assumption was tested with a ^{13}C NMR measurement from a 1:1 molar mixture of PBBf and PBF in TFA-*d*, which yielded peak integrals with 1:1 ratio for the carbons at 68.97 and 68.64 ppm. Accordingly, calculated randomness indices (R_i, Equation 3) point to highly random distributions of both furan-based moieties (R_i values near unity) in the copolyesters.

$$L_{FF} = \frac{A_{FF} + {}^{1}/_{2}(A_{FB}+A_{BF})}{{}^{1}/_{2}(A_{FB}+A_{BF})} \quad (1)$$

$$L_{BB} = \frac{A_{BB} + {}^{1}/_{2}(A_{FB}+A_{BF})}{{}^{1}/_{2}(A_{FB}+A_{BF})} \quad (2)$$

$$R_i = \frac{1}{L_{FF}} + \frac{1}{L_{BB}} \quad (3)$$

Due to similar structural features, the FTIR spectra of all prepared polyesters bear notable resemblance to each other (Figures S3–9). The differences are best illustrated by a direct comparison of PBF and PBBf (Table 2, Figure S11), where several peaks are seen to appear at different wavenumbers and intensities. Prominent features of PBBf are the two intense peaks at 798 and 1444 cm^{-1}, which are not observed in PBF. In addition, instead of the two peaks observed at 3152 and 3119 cm^{-1} in PBF, a single peak is observed in PBBf at 3141 cm^{-1}, with a slight inflection at 3118 cm^{-1}. As expected, these differences can be linked to the motions of the furan rings.[33] Based on simulations, we can further ascribe the differences to certain specific structural features in monomers **1** and **2**

(Table S1). The FTIR spectra of the copolyesters reflect the structural features present in both polyesters, only varying in intensity based on the composition, as expected.

Table 2. Notable FTIR wavenumbers for PBF and PBBf

Wavenumber (cm^{-1})		Assignment
PBF	PBBf	
3153	3141	Furan ν_s(C–H)
3119	3118	Furan ν_{as}(C–H)
2965, 2897	2963, 2897	Methylene C–H
1717	1711	Ester C=O
-	1444	Bifuran ν_s(C=C) + $\delta_{s,ip}$(C–O–C)

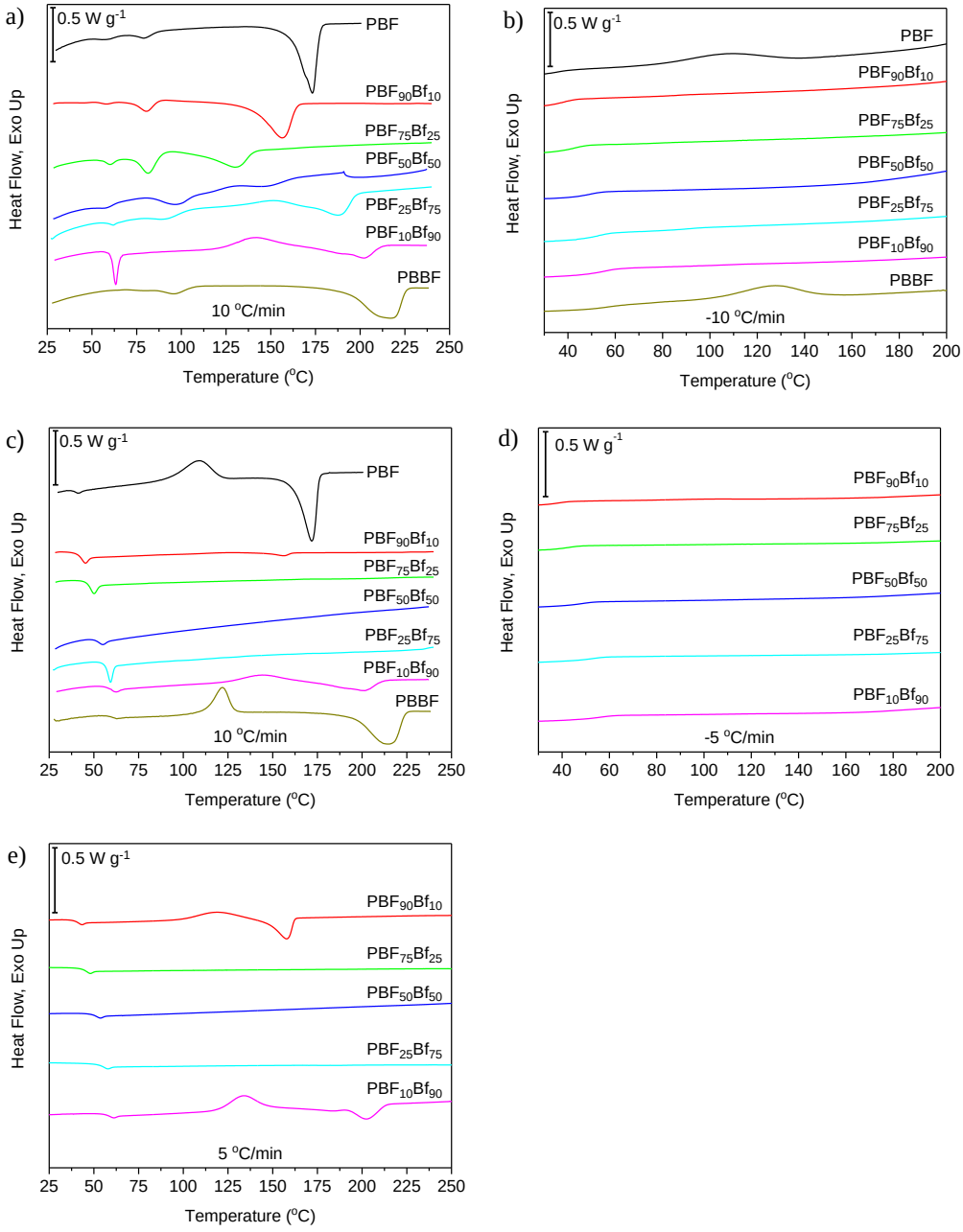

Figure 3. a) 1st heating. b) 1st cooling. c) 2nd heating. d) 1st cooling (copolyesters). e) 2nd heating (copolyesters).

The thermal properties of the dried, methanol-precipitated polyesters were characterized with DSC (melting enthalpies corresponding with Fig. 3 are collected in Table S2). Heating and cooling at 10 °C/min rate shows that both PBF and PBBf are typical semi-crystalline materials with pronounced cold-crystallization and melting peaks (Figure 3a–c, Table 3). The thermal properties of PBF[34] and PBBf[21] also match the previously reported values, though T_g has not been reported for PBBf previously. The copolyesters, on the other hand, lack the pronounced crystallization and melting

peaks. The first heating scans (Figure 3a) do show multiple endothermic peaks (Figure 3a) above T_g, but these disappear in the subsequent heating scan. As all samples were precipitated from solution into methanol and dried for several days at 60 °C, these endothermic peaks likely result from annealing effects. Similar annealing at set temperatures is known to cause multiple melting peaks to appear in similar polyesters such as PBT.[35] The endothermic peaks located at the glass transitions (Figures 3a and 3c) instead result from enthalpic relaxation. Slowing the heating and cooling rates to allow more crystallization to occur only changes the behavior of $PBF_{90}Bf_{10}$ and $PBF_{10}Bf_{90}$ samples (Figures 3c and 3e). Even at the low scanning rate (5 °C/min), neither $PBF_{90}Bf_{10}$ nor $PBF_{90}Bf_{10}$, or the other copolyesters, appear to crystallize from the melt as an exothermic peak is not resolved (Figure 3d). However, $PBF_{90}Bf_{10}$ nor $PBF_{90}Bf_{10}$ samples did cold-crystallize during the subsequent second heating cycle, as evidenced by the exothermic peak before the corresponding endothermic melting peak (Figure 3e). From comparison to the neat polyesters PBF and PBBf, it is obvious that even 10 mol% comonomer incorporation results in hindered crystallization and lowered melting temperatures. Further comonomer incorporation results in inhibition of crystallization, i.e. random copolyesters $PBF_{75}Bf_{25}$, $PBF_{50}Bf_{50}$, and $PBF_{25}Bf_{75}$ appear practically amorphous.

From the data collected into Table 3, it is clear that the bifuran moieties increase the stiffness of the polyester chains, as T_g increases quite linearly with higher bifuran content. Again, for shorter methylene chains in poly(ethylene furanoate) (T_g ~79 °C[34]) and poly(ethylene bifuranoate) (T_g ~107 °C[22]), the bifuran units provided similar T_g enhancement over furan units. In summary, furan or bifuran comonomer incorporation hinders crystallization, but increasing bifuran content results in monotonously increasing T_g. The impact on crystallinity is lower if the content of defects resulting from the incorporation of the minor comonomer is kept relatively small, e.g. below 10 mol%. Compositions approaching 50:50 molar ratio are much more amorphous and are without clear melting events.

Table 3. Thermal properties of PBF, PBBf, and their random copolyesters

Sample	T_g (°C)	T_m (°C)		T_{cc} (°C)	T_{d5} (°C)	T_d (°C)
		1st heating	2nd heating			
PBF	39	173	172	109	366	391
$PBF_{90}Bf_{10}$	43	81, 157	156 (158*)	nd (119*)	365	391
$PBF_{75}Bf_{25}$	49	82, 130	nd	nd	364	392
$PBF_{50}Bf_{50}$	53	97, 145	nd	nd	365	393
$PBF_{25}Bf_{75}$	58	89, 188	nd	nd	367	398
$PBF_{10}Bf_{90}$	60	202	202 (184*, 202*)	144 (134*)	364	397
PBBf	62	217	215	122	370	402

T_g: Glass transition temperature from 2nd heating at 10 °C/min. T_m: Melting temperature from heating at 10 °C/min (*:5 °C/min) T_{cc}: Peak of cold-crystallization from 2nd heating at 10 °C/min (*:5 °C/min). T_{d5}: Temperature at 5% sample mass-loss. T_d: Temperature at peak mass-loss rate. nd: not detected.

Thermogravimetric analysis reveals little variation in the thermal stabilities (Table 3 and Figure 4), the most significant difference arising from the residual weight observed at 700 °C (i.e. char yield). In general, the bifuran content increased the residual weight, while neat PBF had the lowest residual mass (10%). Each polyester composition underwent a single-step decomposition in the range of 391–402 °C, which is close to that of related polyesters, e.g. PET, PBT, and PEF.[36,37] This result indicates that the thermal stabilities are high enough to allow the melts to be processed in similar fashion.

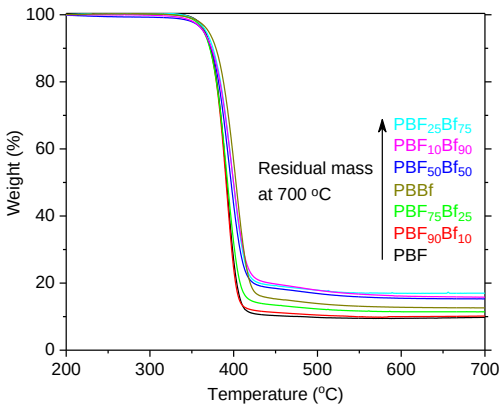

Figure 4. Thermogravimetric decomposition curves for PBF, PBBf, and their random copolyesters under N_2 (heating rate 10 °C/min).

The DMA results (Figure S13) are in a good agreement with the results obtained from DSC. The drop in storage modulus *E*', the peak of loss modulus *E*'' and tan δ all follow the same pattern as the T_g values obtained using DSC, though exactly the same values are not obtained with the different techniques. As can be expected, the polyesters with high T_g retain more of their stiffness at higher

temperatures, e.g. PBBf retains a storage modulus of more than 1 GPa to up to 62 °C, whereas PBF drops below 1 GPa after temperature reaches 32 °C. In DMA, clear cold-crystallization is also observed in PBF, $PBF_{90}Bf_{10}$, and PBBf samples. The corresponding increases in storage moduli begin at roughly 70 °C, 90 °C, and 110 °C, respectively. Other polyester samples are evidently not able to benefit from cold-crystallization, and continue to lose stiffness after 100 °C, having low *E*' values at below 3 MPa.

Another notable feature in the DMA curves is the small size of the tan δ peak for PBF compared to the other polyesters investigated. This suggests a higher crystallinity in PBF initially; despite the broad amorphous halo observed in XRD (Figure S16) consistent with the other samples. Polarized microscopy, coupled with Bertrand lens diffraction, revealed a birefringent pattern due to the presence of spherulites in the melt pressed PBF sample (Figure S14). The melt pressed PBBf sample showed a less clear birefringence due to a very low degree of crystallinity, and the Bertrand lens pattern revealed therefore less developed spherulites. The birefringent pattern in the PBBf sample became significantly clearer after cold crystallization (after the DMA run) and the Bertrand lens pattern indicated more well developed spherulites after the cold crystallization. The birefringent pattern became also clearer after cold crystallization of the PBF sample, due to, as in the case of PBBf, a higher crystallinity.

According to the tensile test data (Table 4), all polyesters were characterized by high rigidity at room temperature. While the E_t was almost constant at around 2 GPa for the range of polyesters, the bifuran units appeared to endow PBBf and the copolyesters with higher tensile strength (≥65 MPa) compared to PBF (59 MPa). In the case of PBF, the mechanical properties can also be compared with previous values found in the literature, though a very wide range of results can be found, e.g. ε_b = 3–200%[38,39,40], most likely due to variations in samples and testing methods (e.g. pressed film instead of an injection molded piece). Our results roughly fall in line with previous characterizations, though

the measured elongation at break is lower than we expected. However, within this test series, PBBf and the copolyesters offered similar or superior mechanical properties compared to PBF.

Table 4. Measured tensile properties of copolyesters

Sample[a]	E_t (GPa)	σ_m (MPa)	ε_b (%)
PBF	2.0±0.1	58.9±2.2	4.0±0.3
$PBF_{90}Bf_{10}$	2.1±0.02	65.1±2.5	4.2±0.2
$PBF_{75}Bf_{25}$	2.0±0.1	66.6±3.1	5.0±0.2
$PBF_{50}Bf_{50}$	2.2±0.1	66.0±1.3	4.3±0.4
$PBF_{25}Bf_{75}$	2.0±0.1	65.8±4.2	5.0±0.2
$PBF_{10}Bf_{90}$	2.1±0.04	65.5±2.7	5.0±0.4
PBBf	2.0±0.1	66.0±3.0	5.4±0.2

[a]At least five amorphous specimens were evaluated for each polyester composition. E_t = Tensile modulus. σ_m = maximum tensile stress. ε_b = elongation at break.

As discussed in the introduction, polyesters derived from FDCA generally have low gas permeability and are considered particularly promising as barrier materials that could replace fossil-based plastics, e.g. PET in some applications. On this basis, O_2 transmission rates of PBF, PBBf, $PBF_{90}Bf_{10}$, and $PBF_{75}Bf_{25}$ were evaluated from melt-pressed, low-crystallinity film specimens (Table 5, entries 1–4). The permeability coefficient for PBF has been reported previously (entry 7), and our sample yielded a somewhat higher value, though they are still in relatively good agreement. Despite the apparent incompatibility of furan and bifuran units in regards to crystallization, it is interesting that the amorphous copolyester films yielded the lowest gas permeability coefficients. It is also important to note that the measured coefficients compare very favorable even against previous data from PET (entries 5 and 6) and PBT (entries 8–10), including data from biaxially oriented, crystalline PBT (entry 10). Comparison to high-performance barrier polyesters poly(ethylene naphthalate) (PEN) and poly(butylene naphthalate) (PBN) shows that further work is still required to challenge these materials: (PEN) is reported to have O_2 permeability as low as 0.008 barrer[41], while bottles made from poly(butylene naphthalate) (PBN) have shown 3x and 6x lower O_2 permeability than PEN and PET bottles, respectively[42]. However, the barrier performance of PEN and PBN comes at a price, since the principal monomer, 2,6-naphthalanedicarboxylic acid, lacks close link to biomass.[43,44]

Based on our results, both FDCA and BFDCA can be almost equally effective for reducing the transmission of oxygen, which is promising for the further development of new bio-based oxygen and gas barrier polymers.

Table 5. O_2 barrier properties of low crystallinity/amorphous PBF, PBBf, $PBF_{90}Bf_{10}$, and $PBF_{25}Bf_{75}$ films.

Entry	Sample	Permeability coefficient (barrer)	Barrier improvement factor vs. PET	Conditions
1	PBF	0.0246±0.0002	2.4–4	
2	$PBF_{90}Bf_{10}$	0.0225±0.0004	2.7–4.4	25 °C at 50% relative humidity (RH)
3	$PBF_{75}Bf_{25}$	0.0217±0.0015	2.8–4.6	
4	PBBf	0.0285±0.0021	2.1–3.5	
5	PET[a]	0.099	1	23 °C, 0% RH
6	PET[b]	0.060	1[b]	30 °C, 50% RH
7	PBF[b]	0.018	3.3[b]	30 °C, 50% RH
8	PBT[c]	0.231	-	23 °C, 50% RH
9	PBT[c,d]	0.0456	-	25 °C, 0% RH
10	PBT[c,e]	0.0258	-	25 °C, 0% RH
11	PEN[f]	0.008	-	23 °C, 50% RH

[a]ref 22. [b]ref 34. [c]ref 45. [d]Unoriented film. [e]Biaxially oriented film. [f]ref 41.

In our previous study, the low UV light transmittance of poly(ethylene bifuranoate) films was discussed as a part of the barrier properties. That in mind, the UV-vis transmittance curves of the various films here were also measured (Figure 5, Table 6). As expected, the bifuran moieties provided the copolyesters intrinsic UV light filtering ability up to about 400 nm wavelengths. The PBF film clearly did not provide significant absorption of UV light in the range of 300–400 nm. PET, often used for its excellent clarity, lacks significant UV-light absorption above 300 nm as well.[22] In the very recent literature, varying strategies for realizing UV-protective green materials have been reported; lignin being a green and bio-based choice.[46,47] However, low transmission at UV wavelengths has been accompanied by low transmission in the visible wavelengths as well due to crystallinity in the aliphatic polyester matrices and most notably the broad absorbance of the lignin used. Here, the strong UV absorption of copolyester films was combined with excellent transmittance values in the visible range (e.g. 82% at 450 nm for $PBF_{90}Bf_{10}$). As discussed previously[21,22], the bifuran monomer **2** has its absorption maximum at longer wavelengths (325 nm) than the furan monomer **1** (265 nm) in chloroform solution (Figure S15). However, in actual melt-pressed polyester

films, the cutoff-wavelength was shifted by almost a 100 nm when enough bifuran moieties were introduced. Most likely, the more conjugated bifuran structures results in more effective chromophore-chromophore interactions with both furan and bifuran units of the polymer chains in solid state that causes the red-shift of absorption. This effect is commonly observed with highly conjugated organic materials.[48] The prepared films with thicknesses of ca. 0.15 mm were remarkably UV-opaque at 10 mol% or higher bifuran content. At a low concentration of 1 mol% ($PBF_{99}Bf_1$ in Figure 5; ^{1}H NMR spectrum in Figure S10), the transmittance at 400 nm is similar to PBF. However, UV opacity was retained in the region of 300–350 nm, which is near the peak absorbance of the bifuran monomer in solution. As a conclusion, the presence of bifuran units in the polymer structure can effectively provide UV filtering ability, reaching the maximum filtration with 1–10 mol% bifuran content for these particular films.

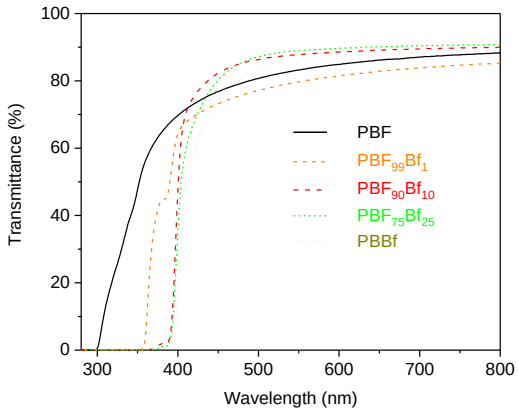

Figure 5. UV-vis transmittance curves of melt-pressed polyester and copolyester films (ca. 0.15 mm thick).

Table 6. UV-vis transmittance values at given wavelengths from Fig. 5.

Sample[a]	T_{350} (%)	T_{380} (%)	T_{400} (%)	T_{450} (%)
PBF	47.7	64.8	69.7	76.8
$PBF_{99}Bf_1$	0.1	44.7	64.2	73.2
$PBF_{90}Bf_{10}$	0	2	47.7	82.3
$PBF_{75}Bf_{25}$	0	1	35.2	80.3
PBBf	0	0.1	13.9	74.5

T_{350} = Transmittance at 350 nm. T_{380} = Transmittance at 380 nm.
T_{400} = Transmittance at 400 nm. T_{450} = Transmittance at 450 nm.

Conclusions

FDCA and BFDCA in combination with 1,4-butanediol were used for the first time to prepare copolyesters, and the properties were compared to the corresponding homopolyesters, PBF and PBBf. In addition, the properties of PBBf were for the first time characterized from melt pressed films, confirming its excellent O_2 barrier properties. The stiff bifuran units in PBBf and the copolyesters endowed them with improved mechanical properties and elevated glass transition temperatures over PBF. The presence of bifuran units also provided intrinsic UV light barrier due to the highly conjugated biheteroaryl moiety, a feature that is not found in PBF. Most notably however, it was shown that the mixtures of furan and bifuran moieties present in the tested copolyesters did not adversely affect the O_2 barrier properties. Instead, the barrier properties were slightly improved compared to either PBF or PBBf. Thus, FDCA-*co*-BFDCA copolyesters were shown function as superior O_2 barriers compared to fossil-based polyesters like PET and PBT. Based on results obtained here, FDCA-*co*-BFDCA polyesters appear to be an interesting class of mechanically strong, semi-crystalline to amorphous materials with combination of excellent oxygen and UV light barrier properties. In addition, the strategy of upgrading C5 sugar-derived furfural into BFDCA, a C10 monomer, appears attractive due to the emerging observations of good properties in bifuran containing polyesters. However, further studies are needed to fully uncover and understand the behavior of BFDCA as a component of different polymers, as this strategy could allow the use of furfural as the feedstock for next generation bio-based polymeric materials.

Associated Content

Supporting Information Available: ^{1}H NMR spectra of dimethyl 2,5-furandicarboxylate and dimethyl 2,2'-bifuran-5,5'-dicarboxylate (Figures S1 and S2), ^{1}H NMR and FTIR spectra for synthesized polyesters (Figures S3–11, Table S1), Melting enthalpies obtained via DSC (Table S2), DMA curves for synthesized polyesters (Figure S13), POM images of PBF and PBBf films (Figure S14), UV-vis absorption spectra for dimethyl 2,5-furandicarboxylate and dimethyl 2,2'-bifuran-5,5'-dicarboxylate

in $CHCl_3$ (Figure S15), XRD-diffractograms of melt-pressed films (Figure S16). This material is available free of charge via the Internet at http://pubs.acs.org.

Author Information

*Corresponding Author: Juha P. Heiskanen. E-mail: juha.heiskanen@oulu.fi

Conflicts of interest

There are no conflicts of interest to declare

Acknowledgements

The Alfred Kordelin foundation and Magnus Ehrnrooth foundation are acknowledged for providing funding. University of Oulu is thanked for providing financial support (Proof of Concept grant). Dr. Tao Hu is thanked for providing guidance in obtaining the XRD data.

References

[1] Bozell, J. J., Petersen, G. R., Technology development for the production of biobased products from biorefinery carbohydrates—the US Department of Energy's "Top 10" revisited. *Green Chem.*, **2010**, *12*, 539–554.

[2] László, T. M., Cséfalvay, E., Németh, Á., Catalytic Conversion of Carbohydrates to Initial Platform Chemicals: Chemistry and Sustainability. *Chem. Rev.*, **2018**, *118*, 505–613.

[3] Mariscal, R., Maireles-Torres, P., Ojeda, M., Sádaba, I., López Granados, M., Furfural: a renewable and versatile platform molecule for the synthesis of chemicals and fuels. *Energy Environ. Sci.*, **2016**, *9*, 1144–1189.

[4] van Putten, R.-J., van der Waal, J. C., de Jong, E., Rasrendra, C. B., Heeres, H. J., de Vries, J. G., Hydroxymethylfurfural, A Versatile Platform Chemical Made from Renewable Resources. *Chem. Rev.*, **2013**, *113*, 1499–1597.

[5] Zeitsch, K. J. *The chemistry and technology of furfural and its many by-products*, Elsevier, 1st edition, 2000.

[6] Sajid, M., Zhao, X., Liu, D. Production of 2,5-furandicarboxylic acid (FDCA) from 5-hydroxymethylfurfural (HMF): recent progress focusing on the chemical-catalytic routes. *Green Chem.*, **2018**, *20*. 5427–5453.

[7] Pan, T., Deng, J., Xu, Q., Zuo, Y., Guo, Q.-X., Fu, Y. Catalytic Conversion of Furfural into a 2,5-Furandicarboxylic Acid-Based Polyester with Total Carbon Utilization. *ChemSusChem*, **2013**, *6*, 47–50.

[8] Zhang, S., Lan, J., Chen, Z., Yin, G., Li, G. Catalytic Synthesis of 2,5-Furandicarboxylic Acid from Furoic Acid: Transformation from C5 Platform to C6 Derivatives in Biomass Utilizations. *ACS Sustainable Chem. Eng.*, **2017**, *5*, 9360–9369.

[9] Zhang, Z., Deng, K., Recent Advances in the Catalytic Synthesis of 2,5-Furandicarboxylic Acid and Its Derivatives. *ACS Catal.*, **2015**, *5*, 6529−6544.

[10] Papageorgiou, G. Z., Papageorgiou, D. G., Terzopoulou, Z., Bikiaris, D. N., Production of bio-based 2,5-furan dicarboxylate polyesters: Recent progress and critical aspects in their synthesis and thermal properties. *Eur. Polym. J.*, **2016**, *83*, 202–229.

[11] Rabnawaz, M., Wyman, I., Auras, R., Cheng, S. A roadmap towards green packaging: the current status and future outlook for polyesters in the packaging industry. *Green Chem.*, **2017**, *19*, 4737–4753.

[12] Margolis, J. M., *Engineering Plastics Handbook*, McGraw-Hill, 1st edition, 2005.

[13] Tachibana, Y., Kimura, S., Kasuya, K., Synthesis and Verification of Biobased Terephthalic Acid from Furfural. *Sci. Rep.*, **2015**, *5*, 8249–8253.

[14] Pang, J., Zheng, M., Sun, R., Wang, A., Wang, X., Zhang, T. Synthesis of ethylene glycol and terephthalic acid from biomass for producing PET. *Green Chem.* **2016**, *18*, 342–359.

[15] Volanti, M., Cespi, D., Passarini, F., Neri, E., Cavani, F., Mizsey, P., Fozer, D. Terephthalic acid from renewable sources: early-stage sustainability analysis of a bio-PET precursor. Green Chem., **2019**, *21*, 885–896.

[16] Burgess, S. K., Leisen, J. E., Kraftschik, B. E., Mubarak, C. R., Kriegel, R. M., Koros, W. J., Chain Mobility, Thermal, and Mechanical Properties of Poly(ethylene furanoate) Compared to Poly(ethylene terephthalate). *Macromolecules*, **2014**, *47*, 1383–1391.

[17] Burgess, S. K., Kriegel, R. M., Koros, W. J., Carbon Dioxide Sorption and Transport in Amorphous Poly(ethylene furanoate). *Macromolecules*, **2015**, *48*, 5184–2193.

[18] Araujo, C. F., Nolasco, M. M., Ribeiro-Claro, P. J. A., Rudić, S., Silvestre, A. J. D., Vaz, P. D., Sousa, A. F., Inside PEF: Chain Conformation and Dynamics in Crystalline and Amorphous Domains. *Macromolecules*, **2018**, *51*, 3515–3526.

[19] Vannini, M., Marchese, P., Celli, A., Lorenzetti, C. Fully biobased poly(propylene 2,5-furandicarboxylate) for packaging applications: excellent barrier properties as a function of crystallinity. *Green Chem.*, **2015**, *17*, 4162–4166.

[20] Wang, J., Liu, X., Jiang, Y., Copolyesters Based on 2,5-Furandicarboxylic Acid (FDCA): Effect of 2,2,4,4-Tetramethyl-1,3-Cyclobutanediol Units on Their Properties. *Polymers*, **2017**, *9*, 305–319.

[21] Miyagawa, N., Ogura, T., Okano, K., Matsumoto, T., Nishino, T., Mori, A. Preparation of Furan Dimer-based Biopolyester Showing High Melting Points. *Chem. Lett.*, **2017**, *46*, 1535–1538.

[22] Kainulainen, T. P., Sirviö, J. A., Sethi, J., Hukka, T. I., Heiskanen, J. P. UV-Blocking Synthetic Biopolymer from Biomass-Based Bifuran Diester and Ethylene Glycol. *Macromolecules*, **2018**, *51*, 1822–1829.

[23] Miyagawa, N., Suzuki, T., Okano, K., Matsumoto, T., Nishino, T., Mori, A., Synthesis of Furan Dimer-Based Polyamides with a High Melting Point. *J. Polym. Sci., Part A: Polym. Chem.*, **2018**, *56*, 1516–1519.

[24] Noordover, B. A. J., van Staalduinen, V. G., Duchateau, R., Koning, C. E., van Benthem, R. A. T. M., Mak, M., Heise, A., Frissen, A. E., van Haveren, J. Co- and Terpolyesters Based on Isosorbide and Succinic Acid for Coating Applications: Synthesis and Characterization. *Biomacromolecules*, **2006**, *7*, 3406-3416.

[25] Yoon, W. J., Hwang, S. Y., Koo, J. M., Lee, Y. J., Lee, S. U., Im, S. S. Synthesis and Characteristics of a Biobased High-T_g Terpolyester of Isosorbide, Ethylene Glycol, and 1,4-Cyclohexane Dimethanol: Effect of Ethylene Glycol as a Chain Linker on Polymerization. *Macromolecules*, **2013**, *46*, 7219−7231.

[26] Wu, J., Eduard, P., Jasinska-Walc, L., Rozanski, A., Noordover, B. A. J., Daan S. van Es, D. S., Koning, C. E. Fully Isohexide-Based Polyesters: Synthesis, Characterization, and Structure−Properties Relations. *Macromolecules*, **2013**, *46*, 384−394.

[27] Mankar, S. V., Garcia Gonzalez, M. N., Warlin, N., Valsange, N. G., Rehnberg, N., Lundmark, S., Jannasch, P., Zhang, B. Synthesis, Life Cycle Assessment, and Polymerization of a Vanillin-Based Spirocyclic Diol toward Polyesters with Increased Glass-Transition Temperature. *ACS Sustainable Chem. Eng.* **2019**, XXXX, XXX, XXX-XXX.

[28] Wang, P., Arza, C. R., Zhang, B. Indole as a new sustainable aromatic unit for high quality biopolyesters. *Polym. Chem.*, **2018**, *9*, 4706–4710.

[29] Duan, R.-T., He, Q.-X., Dong, X., Li, D.-F., Wang, X.-L., Wang, Y.-Z. Renewable Sugar-Based Diols with Different Rigid Structure: Comparable Investigation on Improving Poly(butylene succinate) Performance. *ACS Sustainable Chem. Eng.*, **2016**, *4*, 350−362.

[30] Gruter, G.-J., Sipos, L., Dam, M. A., Accelerating Research into Bio-Based FDCA-Polyesters by Using Small Scale Parallel Film Reactors. *Comb. Chem. High Throughput Screening*, **2011**, *14*, 1–9.

[31] Billmeyer, F. Methods for estimating intrinsic viscosity. *J. Polym. Sci.*, **1949**, *4*, 83–86.

[32] Witt, U., Müller, R.-J., Deckwer, W.-D., Studies on sequence distribution of aliphatic/aromatic copolyesters by high-resolution ^{13}C nuclear magnetic resonance spectroscopy for evaluation of biodegradability. *Macromol. Chem. Phys.*, **1996**, *197*, 1525–1535.

[33] Grigg, R., Knight, J. A., Sargent, M. V. Studies in Furan Chemistry. Part I. The Infrared Spectra of 2,5-Disubstituted Furans. *J. Chem. Soc.*, **1965**, *0*, 6057–6060.

[34] Thiyagarajan, S., Vogelzang, W., Knoop, R. J. I., Frissen, A. E., van Haveren, J., van Es, D. S., Biobased furandicarboxylic acids (FDCAs): effects of isomeric substitution on polyester synthesis and properties. *Green Chem.*, **2014**, *16*, 1957–1966.

[35] Kim, J., Mark E. Nichols, M. E., Robertson, R. E., The annealing and thermal analysis of poly(butylene terephthalate). *J. Polym. Sci., Part B: Polym. Phys.*, **1994**, *32*, 887–899.

[36] Poulopoulou, N., Kasmi, N., Bikiaris, D. N., Papageorgiou, D. G., Floudas, G., Papageorgiou, G. Z., Sustainable Polymers from Renewable Resources: Polymer Blends of Furan-Based Polyesters. *Macromol. Mater. Eng.*, **2018**, *303*, 1800153–1800160.

[37] Morales-Huerta, J. C., Martínez de Ilarduya, A., Muñoz-Guerra, S., Sustainable Aromatic Copolyesters via Ring Opening Polymerization: Poly(butylene 2,5-furandicarboxylate-co-terephthalate)s. *ACS Sustainable Chem. Eng.*, **2016**, *4*, 4965−4973.

[38] Wu, L., Mincheva, R., Raquez, J.-M., Dubois, P. High Molecular Weight Poly(butylene succinate-co-butylene furandicarboxylate) Copolyesters: From Catalyzed Polycondensation Reaction to Thermomechanical Properties. *Biomacromolecules*, **2012**, *13*, 2973–29981.

[39] Wu, B., Xu, Y., Bu, Z., Li, B.-G., Dubois, P., Biobased poly(butylene 2,5-furandicarboxylate) and poly(butylene adipate-co-butylene 2,5-furandicarboxylate)s: From synthesis using highly purified 2,5-furandicarboxylic acid to thermo-mechanical properties. *Polymer*, **2014**, *55*, 3648–3655.

[40] Wang, J., Liu, X., Zhu, J., Jiang, Y., Copolyesters Based on 2,5-Furandicarboxylic Acid (FDCA): Effect of 2,2,4,4- Tetramethyl-1,3-Cyclobutanediol Units on Their Properties. *Polymers*, **2017**, *9*, 305–319.

[41] Lange, J., Wyser, Y., Recent Innovations in Barrier Technologies for Plastic Packaging – a Review. *Packag. Technol. Sci.*, **2003**, *16*, 149–158.

[42] Kulkarni, S. T., Bisht, H., Lakshminarayanapuram, R. S. Gas barrier PET composition for monolayer bottle and process thereof. US Patent Application US 20060182911 A1, Aug 17, 2006.

[43] Elman, A. R. Synthesis Methods for 2,6-Naphthalenedicarboxylic Acid. *Catal. Ind.*, **2009**, *1*, 184–189.

[44] Ban, H., Cheng, Y., Wang, L., Li, X., Zhou, X., Zhang, X. Preparation of High-Purity

2,6-Naphthalenedicarboxylic Acid from Coal Tar Distillate. *Chem. Eng. Technol.*, **2019**, *42*, 1188–1198.

[45] McKeen, L. W. *Permeability Properties of Plastics and Elastomers*, Elsevier, 4th edition, 2017

[46] Xing, Q., Ruch, D., Dubois, P., Wu, L., Wang, W.-J., Biodegradable and High-Performance Poly(butylene adipate-*co*-terephthalate)−Lignin UV-Blocking Films. *ACS Sustainable Chem. Eng.*, **2017**, *5*, 10342−10351.

[47] Xing, Q., Buono, P., Ruch, D., Dubois, P., Wu, L., Wang, W.-J., Biodegradable UV-Blocking Films through Core−Shell Lignin−Melanin Nanoparticles in Poly(butylene adipate-*co*-terephthalate). *ACS Sustainable Chem. Eng.*, **2019**, *7*, 4147−4157.

[48] Sippola, R. J., Hadipour, A., Kastinen, T., Vivo, P., Hukka, T. I., Aernouts, T., Heiskanen, J. P., Carbazole-based small molecule electron donors: Syntheses, characterization, and material properties. *Dyes and pigments*, **2018**, *150*, 79–88.